https://doi.org/10.15407/ujpe67.11.811

HAMZA A. MEZHER, KADHIM AL-ATTAFI, BASHAR ALKOTBE, WISAM N. HUSSEIN

Department of Physics, College of Science, University of Kerbala
(Karbala, Iraq; e-mails: hamza.a@uokerbala.edu.iq, kadhim.m@uokerbala.edu.iq, bashar.alal@uokerbala.edu.iq, wisam.n@uokerbla.edu.iq)

INVESTIGATION OF THE CROSS-SECTIONS FOR THE PRODUCTION OF BROMINE ISOTOPES USING PROTON-INDUCED REACTIONS

We have considered the production of bromine isotopes by studying the cross-sections of nuclear reactions in the selenium-enriched target. This is of importance due to the applications in nuclear medicine and radiation therapy. Eight channels are observed in the production of bromine isotopes: ${}^{76}_{34}Se(p,2n)\ {}^{75}_{35}Br$, ${}^{77}_{34}Se(p,3n)\ {}^{75}_{35}Br$, ${}^{76}_{34}Se(p,n)\ {}^{76}_{35}Br$, ${}^{77}_{34}Se(p,2n)\ {}^{76}_{35}Br$, ${}^{77}_{34}Se(p,n)\ {}^{77}_{35}Br$, ${}^{78}_{34}Se(p,2n)\ {}^{77}_{35}Br$, ${}^{80}_{34}Se(p,4n)\ {}^{77}_{35}Br$, *and* ${}^{80}_{34}Se(p,n)\ {}^{80m}_{35}Br$. *The energy of the interacting protons ranging from the threshold is 2.20–84.20 MeV and is calculated by using an activation technique. For the proton-induced production of bromine isotopes from selenium target atoms, the stopping power and the yield have been calculated. The Zeigler formula was applied to investigate the cross-sections and to determine the yield for each reaction over the stopping power range. The total energy of each reaction and the corresponding cross-sections are statistically analyzed. These energies are reproduced by the incident proton energy with acceptable errors at 0.01 MeV intervals. One of the most significant results of the current calculations is the stopping power of targets evaluated within the Ziegler and SRIM approaches.*

K e y w o r d s: cross-section, Zeigler formula, stopping power, selenium-enriched target, bromine yield.

1. Introduction

Due to the kinetic energy of the accelerated nucleus, two nuclei with different potentials can become close to each other and can interact. In view of many important applications of bromine isotopes, in particular, in the medical fields, the proton interaction technique was used with the nuclei of selenium-enriched targets for the production of these isotopes. In the current era, the use of radioactive isotopes is essential in various fields of life science. The most widely used radionuclides in nuclear medicine are radioactive isotopes, which are utilized to create radiopharmaceuticals from unique chemical complexes [1]. Positron Emission Tomography (PET) and Single-Photon Emission Computed Tomography (SPECT) are considered the unique utilization of radionuclides for diagnostic medical purposes. Furthermore, it is becoming increasingly important in internal radiotherapy. Because of the increasing demand for neutrons, the lack of radioactive isotopes, and their low cost, models of the therapeutic cyclotron equipment were intensively developed. In recent years, the benefit of accelerators was enhanced considerably, and nuclear reactors were used in the production of isotopes. Physicians employed radionuclides to investigate non-invasively various ailments. These radionuclides allow a radiologist to chart the illnesses and

assess the heart function of patients using external radiation detectors [2]. Recently, some alternative production techniques have been studied due to the high cost of the enriching elements. Because radioactive isotopes have been currently used in a lot of medical applications, there is a greater need for effective radioactive isotopes. The identification of the cross-sections of nuclear reactions on a wide energy scale is considered a critical step in the establishment of optimum conditions of production methods. This significantly contributes to the development of the nuclear models. The process of producing radionuclides and their half-lifes can be found in Table 1. The cross-section of the proton-induced reactions on the nuclei of selenium atoms which produce bromine isotopes are presented in the International Atomic Energy Agency (IAEA) libraries, and other published empirical information sources [3, 4]. Commonly, the interaction mechanism relies on the interaction between the target (nucleus) and the particle (proton). These interactions can be divided into scattering operations and nuclear ones. When fast charged particles pass through the material, they collide inelastically with ions, atoms, or molecules of this material. The energy of the incident particles, as well as the characteristics of the material which is passed through, affect their stopping power. To produce bromine isotopes from selenium, a certain numbers of identical atoms were investigated for the high-power analysis up to energies that are available at conventional accelerators. For any thickness of a target, the yield is referred to the ratio between the number of nuclei produced during a nuclear reaction and the number of particles striking the target. The recommended cross-section presented in this work for a target with a significant thickness was utilized to examine the calculated yields in [5, 6]. The cross-sections reactions were produced inaccurately for 0.01-MeV increments of the declining proton energy, and the accompanying inaccuracies were incorporated into the suggested estimated values. In the current work, authors' data were used [19–32] within the energy interval 2.20–84.20 MeV. The calculated yields of the proton-induced reactions to create bromine isotopes from selenium atoms are presented on the plots. The cross-section activation data at intermediate energies have gained increasing importance for a wide range of distinctive uses [7].

2. Theoretical Part

2.1. Stopping power

Recently, the importance of the theoretical study of the stopping power and the range of molecules in different materials has increased dramatically. Due to the perpetual collisions of charged particles with elements of a target, these particles will gradually lose their energy. Ziegler used a method to extract the combined terminology of adjustment for the normalizing of stop computations for interactions to analyze the various types of energy. Three ranges of energies (low, middle, and high) can be applied to explain the behavior of ions in each energy area. The particle velocity, charge, and type of material all play a role in the mechanism determining the stopping power for atoms that penetrate materials [8].

2.1.1. The low-energy region

The Thomas–Fermi potential is used to calculate the electronic stopping cross-section as a function of the particle velocity within a region (ϑ) ($\vartheta < \vartheta_0 Z_1^{2/3}$). The equation that describes this region is given by:

$$S_e = 8\pi e^2 a_0 \frac{Z_1^{7/6} Z_2}{Z^{2/3}} \left(\frac{\vartheta}{\vartheta_0}\right), \tag{1}$$

where

$$Z^{2/3} = Z_1^{2/3} + Z_2^{2/3}, \tag{2}$$

and a_0 represents the Bohr radius

$$a_0 = \frac{h^2}{me^2} = 5.29 \times 10^{-11} \text{ Å}. \tag{3}$$

In this study, the program used to calculate the electronic stopping power for the experimental methods presented by Ziegler is represented by the following equations [9]:

1. Energy spectrum (1–10) $\times 10^{-3}$ keV

$$-\frac{dE}{dx} = A_1 E^{1/2}. \tag{4}$$

2. Energy spectrum (10–999) $\times 10^{-3}$ keV

$$\left(-\frac{dE}{dx}\right)^{-1} = \left(-\frac{dE}{dx}\right)_{\text{Low}}^{-1} + \left(-\frac{dE}{dx}\right)_{\text{High}}^{-1}, \tag{5}$$

$$\left(-\frac{dE}{dx}\right)_{\text{Low}} = A_2 E^{0.45}, \tag{6}$$

$$\left(-\frac{dE}{dx}\right)_{\text{High}} = \left(\frac{A_3}{E}\right) \ln\left[1 + \left(\frac{A_4}{E}\right) + A_5 E\right]. \tag{7}$$

3. Energy spectrum (1000–100.000) $\times 10^{-3}$ keV

$$\left(-\frac{dE}{dx}\right) = \left(\frac{A_6}{\beta^2}\right)\left[\ln\left(\frac{A_7\beta^2}{1-\beta^2}\right) - \beta^2 - \right.$$

$$\left. - \sum_{i=0}^{4} A_{i+8}(\ln E)^i\right]. \quad (8)$$

We also found that: A_i is the Ziegler coefficient, E is the energy of particles in MeV, B is the ratio between the speed of the incident particle and the speed of light [10, 11].

2.1.2. The middle energy region

When the velocity of the incident particle (ϑ) falls into the interval ($2\vartheta_0 Z_1 > \vartheta \geqslant \vartheta_0 Z_1^{2/3}$), it has the greatest stopping power. This occurs in the medium energy area. As a result of the loss of the charged particle energy, this leads to a decrease in their velocity and charge Z_1, and atoms' nuclei will collide elastically due to the loss and gain of the same energy by electrons. Thus, the effect of the active charge will be evident in this region. Equation (1) and the electronic stopping power were thus adjusted as in the Bethe–Bloch model (1933):

$$-\frac{dE}{dx} = NS_e = \frac{4\pi K^2 e^4 Z_1^2}{m\vartheta^2} N Z_2 L, \quad (9)$$

$$L = L_0 + Z_1 L_1 + Z_1^2 L_2. \quad (10)$$

While (L), which depends on the particle velocity and the target material, is known as the stopping atomic number, where,

$$L_0 = \ln(2wv^{1/2}/I) - C/Z_2, \quad (11)$$

($Z_1 L_1$) is the correction of Barka's influence of polarization, ($Z_1^2 L_2$) is Bloch's correction to the conversion from the quantum to classical description, C/Z_2 is the shell correction [12].

2.1.3. The high-energy region

It is the resulting zone, when the speed of the incident particle is around ($V \geqslant 2V_0 Z_1$). Since ions moving at speeds below (V_0) constantly collide with the target electrons, their stopping force is low. As a result, the stopping force increases as the ionic velocity decreases. The dominant equation for calculating the electronic stopping power in this region is the Bethe one (1933):

$$-\frac{dE}{dx} = NS_e = \frac{4\pi K^2 e^4 Z_1^2}{m\vartheta^2} \times$$

$$\times N Z_2 \left[\ln\left(\frac{2m\vartheta^2}{I}\right) - \ln\left(1-\beta^2\right) - \beta^2\right], \quad (12)$$

where: V_0 is the Bohr velocity ($V_0 = 2.18 \times 10^6$ m/s), N is material's atomic density [$N = N_a\ (\rho/A)$]. N_a is Avogadro's number ($N_a = 6.022 \times 10^{23}$ mole^{-1}), ρ is the material density, A is the mass number, e and m are the electron's charge and mass, respectively, Z_1 and Z_2 are the atomic numbers of the ion and the target, respectively, β is the ratio of the speed of the incident particle to the speed of light

$$\beta = \frac{\vartheta}{c},$$

I is the typical ionization and excitation potential, $K = \frac{1}{4\pi\varepsilon_0} = 8.99 \times 10^9$ Nm^{2}C^{-2} [13].

2.2. Yield calculations

To make the calculations of the yield per particle (Y) for the ideal delicate target, we consider the monoenergetic inicdent particle:

$$Y = (nt)\,\sigma\,(E_b)\,\varepsilon\,(E_b), \quad (13)$$

where n selects the desired number of atoms per volume unit, t is the target thickness, σ is the cross-section of the interaction, ε is the efficiency to reveal a proton, E_b is the incident energy.

Regarding the infinitely thick target and the relationship between the calculated yield and the loss in energy during passing through the target, we can write the relation:

$$Y = \int_{E_{\rm thr}}^{E_b} \frac{n\,\sigma\,(E)\;\varepsilon\;(E)\,f dE}{-\frac{dE}{dx}\,(E)}, \quad (14)$$

where ($E_{\rm thr} = E_b - \Delta E$), $E_{\rm thr}$ is the threshold energy, ΔE is the beam's energy loss at a target, f is the number of target atoms present in each target molecule, $-\frac{dE}{dx}\,(E)$ is a function of the beam energy and the stopping power of the target.

If each molecule has one atom (i.e., $f = 1$) and considering the efficiency $\varepsilon\,(E) = 1$, it can be said

Table 1. **International libraries were utilized to acquire the most accurate measurement data for induced proton effects on selenium isotopes**

Target element	Reaction		Target element	Reaction	
	Library	Product		Library	Product
$^{76}_{34}$Se	EXFOR	(p,2n)$^{75}_{35}$Br	$^{77}_{34}$Se	EXFOR	(p,n)$^{77}_{35}$Br
	EXFOR	(p,n)$^{76}_{35}$Br	$^{78}_{34}$Se	EXFOR	(p,2n)$^{77}_{35}$Br
$^{77}_{34}$Se	EXFOR	(p,3n)$^{75}_{35}$Br	$^{80}_{34}$Se	EXFOR*	(p,4n)$^{77}_{35}$Br
	EXFOR	(p,2n)$^{76}_{35}$Br		EXFOR	(p,n)$^{80}_{35}$Br

*Only one author gives data. EXFOR: Exchange Format.

that the target is thick enough. The calculated yield is given by the relation:

$$Y(E_b) = \int_{E_{\text{thr}}}^{E_b} \frac{n\sigma(E)\,dE}{-(dE/dx)}. \tag{15}$$

But the stopping power is as follows: $\frac{1}{n}\left(-\frac{dE}{dx}\right)$ [14–17].

2.3. Reduction and analysis of data

The methods presented below were used to obtain the recommended cross-sections:

1) Gathering empirical cross-sectional data for various authors and different energy intervals. The cross-sections are rearranged with errors identical for the 0.01 MeV energy interval.

2) The statistical distribution of cross-sectional errors was normalized for the normal cross-section values for each author.

3) The internal completion of the closest data for each power period was carried out using the Matrix Laboratory (Matlab-7.0 program) as a result of the errors associated with cross sections.

4) The following relations were derived using the interpolated data to reach the weighted average that provides the basis for the adopted cross-section:

$$\sigma_{\text{w.a.}} = \frac{\sum_{i=1}^{n} \frac{\sigma_i}{(\Delta\sigma_i)^2}}{\sum_{i=1}^{n} \frac{1}{(\Delta\sigma_i)^2}}. \tag{16}$$

The error value for the standard deviation is written as:

$$\text{S.D.} = \frac{1}{\sqrt{\sum_{i=1}^{N} \frac{1}{(\Delta\sigma_i)^2}}}, \tag{17}$$

where σ_i is cross section value. $\Delta\sigma_i$ is the corresponding error for each cross-section [18].

2.4. Computational details

To conduct a theoretical study using the nuclear reactions that result in the decay of the composite nucleus into discrete and continuous states, the equilibrium calculations have been performed by using the Matlab program.

It includes calculations of the total cross-sections and cross-sections of the compound nuclei consisting of (P, X) interactions that give radioactive bromine nuclei as products, where scientific data are available for the permissible energy range from the threshold energy of the proton. The practically measured cross-sections are based on the International Atomic Energy Agency libraries (IAEA) such as Exchange Format Data (EXFOR), Q-Value, Threshold energy, Production Yield, Activity, and Width can be calculated and compared with the approved practical values.

3. Results and Discussions

This study involves recommended cross-sections utilizing the Matlab 7.0 program. The used data were obtained from the EXFOR library, to calculate the yield for the proton incident on the selenium-enriched target. The evaluated cross-sections for the production of bromine isotopes are given in Table 1. The results concerning the cross-section of the nuclear reactions are as follows.

3.1. ^{76}Se(p,2n)^{75}Br reaction

To determine the cross-section of the reaction ^{76}Se(p,2n)^{75}Br, according to Fig. 1, we used two sets of data published by A.M.J. Paans *et al.* (1980) [19] and Z. Kovacs *et al.* (1985) [20] that have threshold energies estimated from 15.74 up to 39.85 MeV. That

is, the cross-sectional data available for the second reaction are related to an energy greater than 30 MeV. The process of decreasing the cross-section is a function of the energy of the proton incident on the ^{76}Se target in the (p,2n) reaction and can be used to produce the ^{75}Br isotope.

3.2. $^{77}Se(p,3n)^{75}Br$ reaction

The second reaction of the bromine isotope production ^{75}Br is (p,3n) for a proton incident on a nucleus of ^{77}Se. It is formed by two sets of data and published by the authors Levkovskij *et al.* (1991) [21] and Spahn *et al.* (2009) [22] and has the threshold energy ranging from 24.00 up to 56.60 MeV as shown in Fig. 2.

3.3. $^{76}Se(p,n)^{76}Br$ reaction

The ^{76}Se(p,n)^{76}Br reaction, whose threshold energy is 4.60 up to 39.88 MeV, is presented in Fig. 3. Cross-section data for this nuclear reaction at low energies, as written by Paans *et al.* (1980) [19], Kovacs *et al.* (1985) [20], Levkovskij *et al.* (1991) [21] and Hassan *et al.* (2004) [23], have been plotted and interpolated to get the recommended cross-sections for this reaction.

3.4. $^{77}Se(p,2n)^{76}Br$ reaction

The second important interaction for the production of the isotope of bromine ^{76}Br is (p,2n) which includes the proton incident on the ^{77}Se target. We have used the data on the cross sections which consist of four sets from four sources, namely Janssen *et al.* (1980) [24], Levkovskij *et al.* (1991) [21], Hassan *et al.* (2004) [23] and Spahn *et al.* (2009) [22]. These data reveal the threshold energies from 6.70 up to 56.60 MeV of the nuclear reactions producingr the ^{76}Br isotope.

3.5. $^{77}Se(p,n)^{77}Br$ reaction

As for the cross-section of the nuclear (p,n) reaction for a proton incident on the selenium target to produce the isotope of bromine, which consists of eight sets of data and published by eight authors, namely Johnson *et al.* (1960) [25], Fedorets *et al.* (1977) [26], Skakun *et al.* (1980) [27], Janssen *et al.* (1980) [24], Levkovskij *et al.* (1991) [21], Skakun *et al.* (1992) [28], Hassan *et al.* (2004) [23], and Spahn *et al.* (2010) [29] that have the threshold energy estimated from 2.19 up to 56.60 MeV. The (p,n) reaction that creates the ^{77}Br isotope is regarded as one of the most significant nuclear reactions.

3.6. $^{78}Se(p,2n)^{77}Br$ reaction

The second important reaction is (p,2n) to produce ^{77}Br isotope from the ^{78}Se target which is within the higher energy rof the incident proton, as it has threshold energy ranging from 13.80 up to 64.70 MeV. The

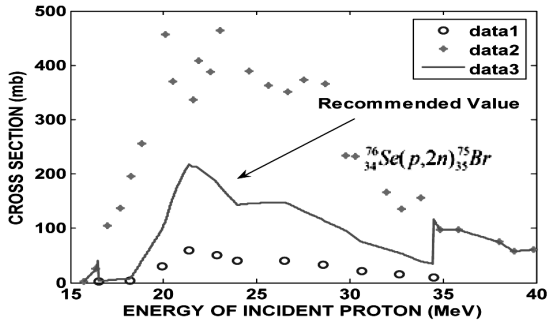

Fig. 1. The recommended cross-sections for the $^{76}_{34}$Se target (present work) compared with EXFOR Library. Data 1: Ref. [19]; Data 2: Ref. [20]; Data 3: (PW)

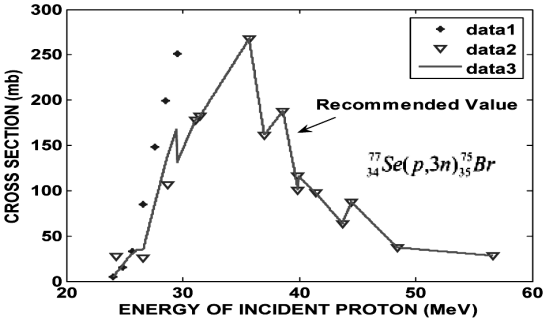

Fig. 2. The recommended cross-sections for the $^{77}_{34}$Se target (present work) compared with EXFOR Library. Data 1: Ref. [21]; Data 2: Ref. [22]; Data 3: (PW)

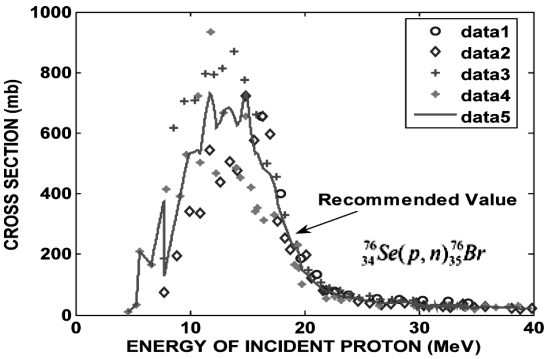

Fig. 3. The recommended cross-sections for the $^{76}_{34}$Se target (present work) compared with EXFOR Library. Data 1: Ref. [19]; Data 2: Ref. [20]; Data 3: Ref. [21]; Data 4: Ref. [23]; Data 5: (PW)

data were published by three groups: Janssen *et al.* (1980) [24], Levkovskij *et al.* (1991) [21], and Spahn *et al.* (2010) [29], as shown in Fig. 6.

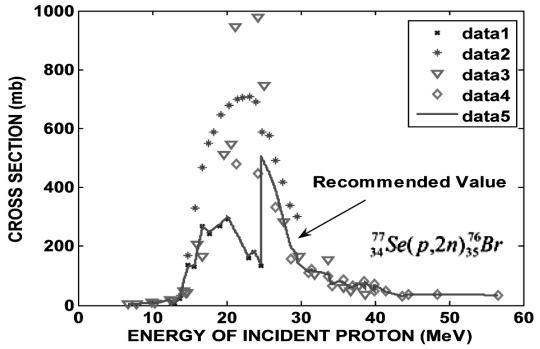

Fig. 4. The recommended cross-sections for the $^{77}_{34}$Se target (present work) compared with EXFOR Library. Data 1: Ref. [24]; Data 2: Ref. [21]; Data 3: Ref. [23] Data 4: Ref. [22]; Data 5: (PW)

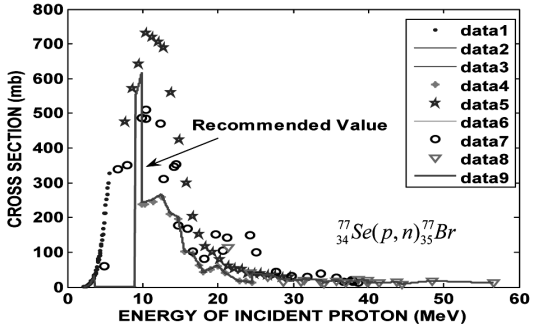

Fig. 5. The recommended cross-sections for the $^{77}_{34}$Se target (present work) compared with EXFOR Library. Data 1: Ref. [25]; Data 2: Ref. [26]; Data 3: Ref. [27] Data 4: Ref. [24]; Data 5: Ref. [21]; Data 6: Ref. [28] Data 7: Ref. [23]; Data 8: Ref. [29]; Data 9: (PW)

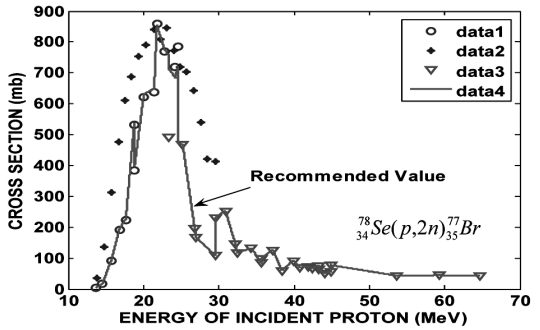

Fig. 6. The recommended cross-sections for the $^{78}_{34}$Se target (present work) compared with EXFOR Library. Data 1: Ref. [24]; Data 2: Ref. [21]; Data 3: Ref. [29] Data 4: (PW)

3.7. ^{80}*Se(p,4n)*^{77}*Br reaction*

The final reaction producing the isotope ^{80}Br is (p,4n) for a proton incident on the ^{78}Se target. It is less important, because it occurs in regions of high energies, where the energy threshold is from 34.50 up to 84.20 MeV, The data are raken from the following works: Spahn *et al.* (2010) [29], as shown in Fig. 7.

3.8. ^{80}*Se(p, n)*^{80m}*Br reaction*

The reaction (p,n) to produce the isotope ^{80}Br from the ^{80}Se target is considered as the most significant due to its importance in medical applicatiobs. It can also occur within low-energy regions, where the threshold energy ranges from 2.67 up to 18.50 MeV. We have used seven sets of data: Blaser *et al.* (1951) [30], Johnson *et al.* (1964) [31], Kailas *et al.* (1979) [32], Skakun *et al.* (1980) [27], Levkovskij *et al.* (1991) [21], Skakun *et al.* (1992) [28] and Spahn *et al.* (2010) [29], as shown in Fig. 8.

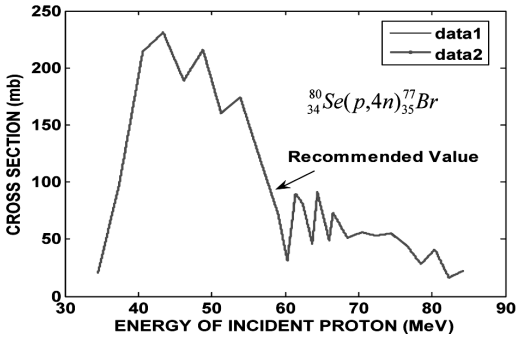

Fig. 7. The recommended cross-sections for the $^{80}_{34}$Se target (present work) compared with EXFOR Library. Data 1: Ref. [29]; Data 2: (PW)

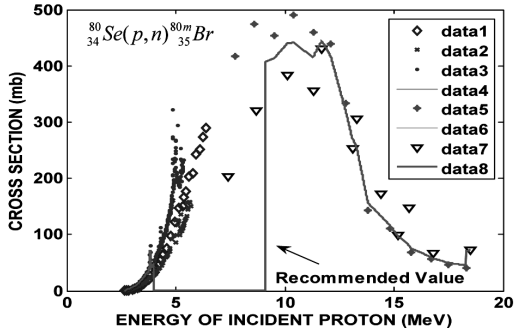

Fig. 8. The recommended cross-sections for $^{80}_{34}$Se target (present work) compared with EXFOR Library. Data 1: Ref. [30]; Data 2: Ref. [31]; Data 3: Ref. [32] Data 4: Ref. [27]; Data 5: Ref. [21]; Data 6: Ref. [28]; Data 7: Ref. [29]; Data 8: (PW)

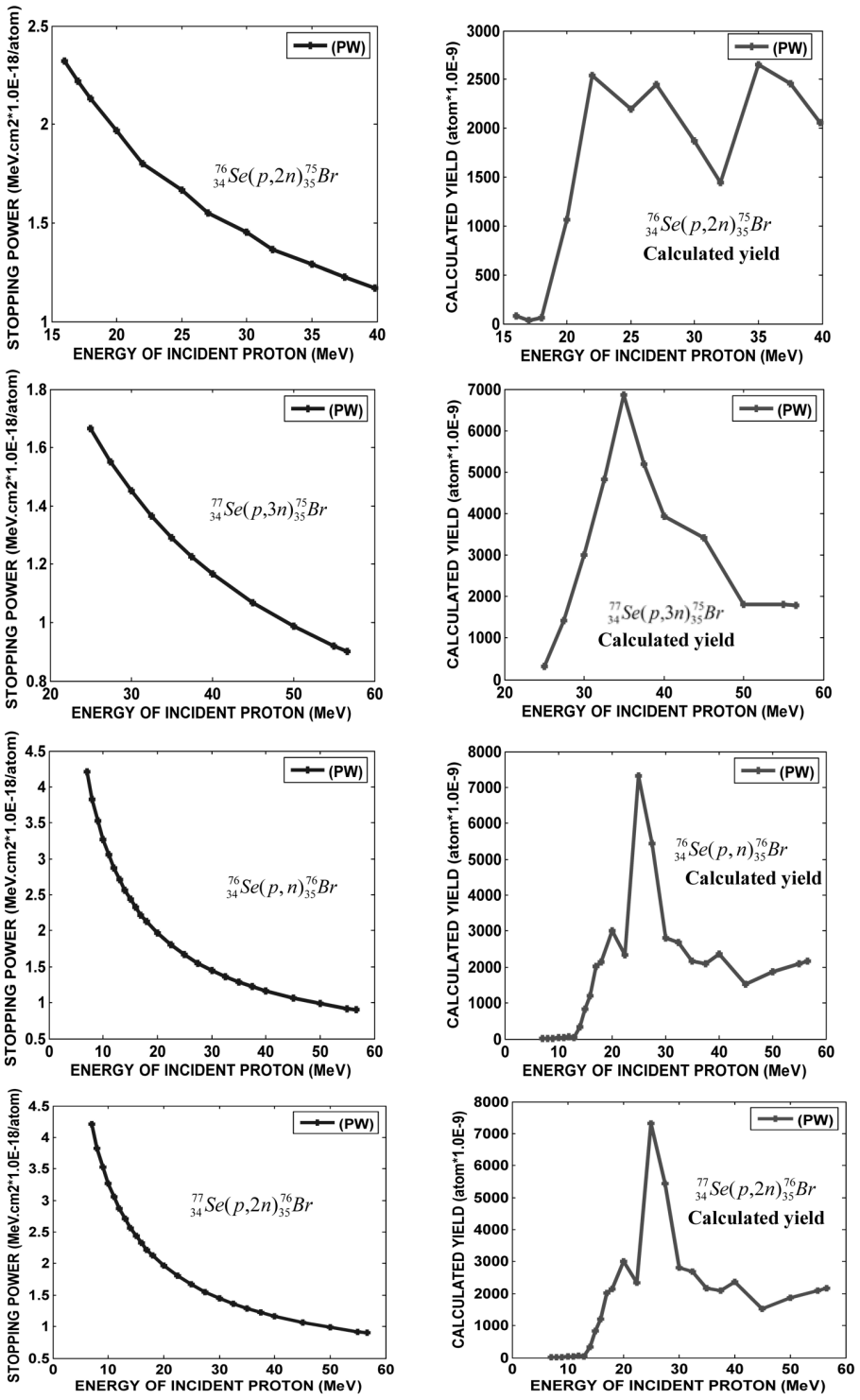

Fig. 9. Left side; calculated and SRIM (2003) stopping power verses the incident proton energy on ^{35}Se. Right side; calculated and experimental yields based on the adopted cross-sections for the ^{35}Se reaction with a proton

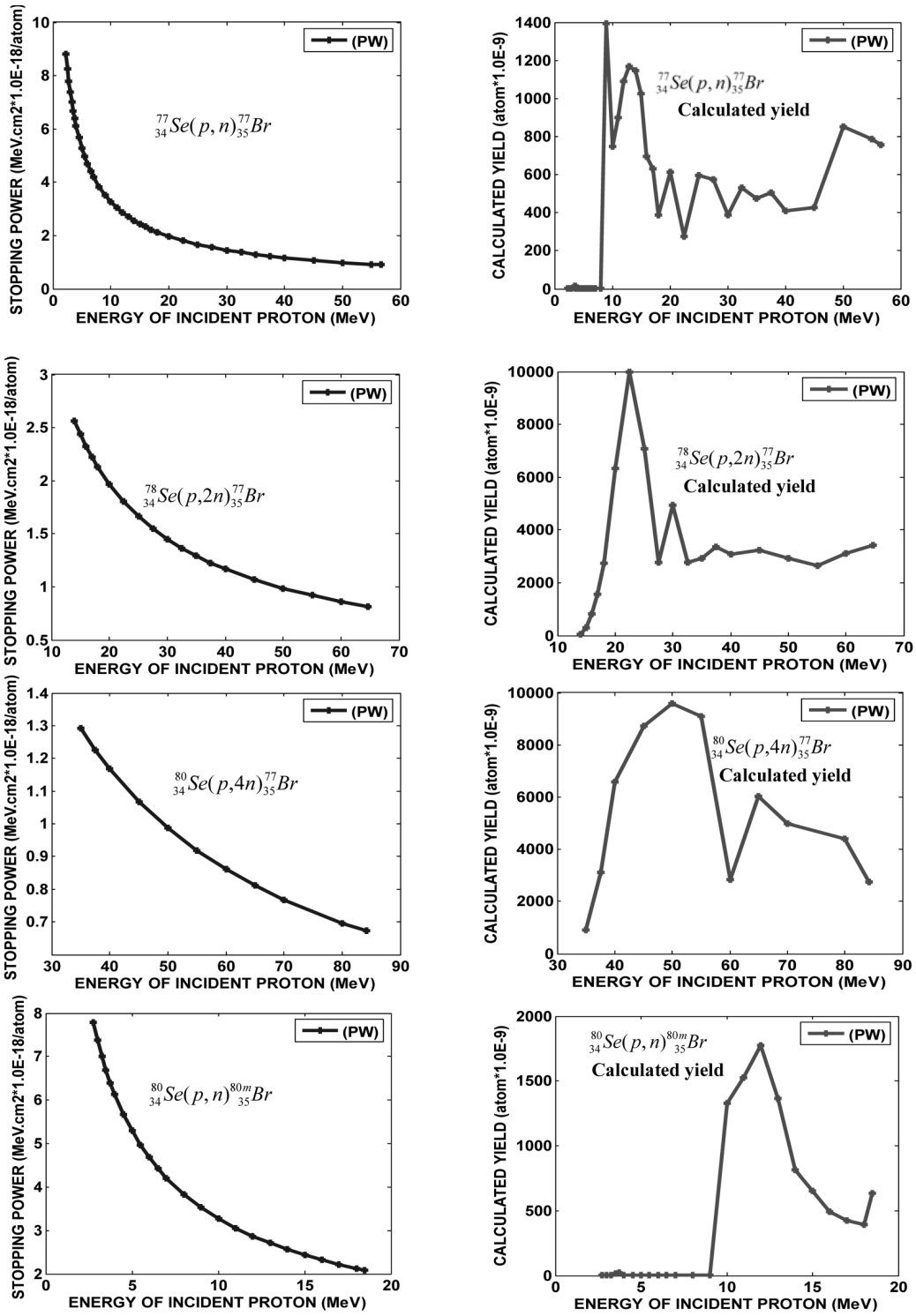

Fig. 10. The stopping energy versus the energy of an incident proton and their corresponding calculated yield

Table 2. **Ziegler coefficients for the proton [15]**

Target element	A-1	A-2	A-3	A-4	A-5	A-6	A-7	A-8	A-9	A-10	A-11	A-12
H	1.262	1.440	242.6	1.2E + 04	0.1159	0.0005	54360	–5.05	2.049	–0.3044	0.0196	–0.0004
Se	5.874	6.656	7395	117.51	0.0076	0.0173	3006	–13.11	4.965	–0.6735	0.0393	–0.0008
Br	5.611	6.335	8046	365.2	0.0062	0.0178	2928	–13.40	5.083	–0.6906	0.0402	–0.0008

We note that, when analyzing the results of a proton-induced reaction on the selenium target for the production of bromine isotopes, we indicate that separate nuclear states are characterized as eligible for the normal dissolution and have a width, half-life, and distinct separations. The overlap between the energy distributions of two various states is very undesirable as it leads to confusion for the decay's resulting steady-state and, consequently, for calculating the cross-sections at the specific energy of the incident protons and for the nuclear state.

We may conclude that unstable states that are not characterized by exact wave functions, because they are strongly intertwined and mixed. The width in these cases is small compared to their separation. The instability of the complex nuclei results in the inaccuracy in determining the energy levels. In this work, the Ziegler method, experimental formulas, and the Ziegler coefficients were used as theoretical outcomes to account for the stopping power of the targets for protons, as shown in Table 2:

In the energy range (1–10) keV/amu, we use coefficients A-1.

But, in the energy range (10–999)keV/amu, we took coefficients A-2 to A-5.

For the energy levels higher than 1000 keV/amu, we use coefficients A-6 to A-12.

Thus, as for the production of Br isotopes from selenium, the calculated cross-sections of each nuclear reaction are of great importance for calculating the yields used in diagnosis, nuclear medicine, and drug production. The most significant isotopes studied in this research are bromine 75, 76, 77, and 80. They can be discussed as follows:

1. Isotopes $^{75}_{35}$Br and $^{76}_{35}$Br have half-life (1.61 and 16.20) hour , respectively. The isotope $^{75}_{35}$Br is considered one of the most important isotopes used in rapid metabolism processes, as it is a positron emitter and can be applied in (PET), in addition to its importance in the field of nuclear medical [19]. As for the isotope ^{76}Br, it has been utilized, in particular, in the PET imaging for a long time because of its appropriate half-life and modern work [4, 20].

2. Isotopes $^{77}_{35}$Br and $^{80m}_{35}$Br have half-lives (57.04 and 4.40) hour, respectively. These isotopes are distinguished by the results of their interactions with the emission of two Auger electrons, and one of its most important applications in internal nuclear therapy [21, 22]. Through low-energy (p,n), (p,2n) and (p,4n) interactions and for the production of the $^{77}_{35}$Br isotope, the cross-sectional data have been identified $^{77,78,80}_{34}$Se targets have been used. These calculations have been expanded by studying nuclear processes. The isotope $^{80m}_{35}$Br is only produced through the reaction (p,n) in the target $^{80}_{34}$Se. This isotope can be used to produce therapeutic radionuclides [23].

With the increase in the incident proton energy, the stopping power gradually diminishes. Filled outer shells increase a calculated increase, which enhances the possibility of bromine isotope production due to the irradiation of the selenium-enriched target with protons. It is clear from the results obtained and from the figures drawn that the stopping powers for the two reactions ^{77}Se(p,n)^{77}Br and ^{80}Se(p,n)^{80}Br are 8.86 and 7.79 (MeV $\cdot$ cm^2*1.0E-18/atom) at proton energies 2.56 and 2.49 MeV, respectively [18].

In this research, we also calculated the yield and concluded that it increases with the energy of the proton. We mention the higher calculated yield for two reactions ^{78}Se(p,2n)^{77}Br and ^{80}Se(p,n)^{77}Br that are 9996 and 9785 (atom*1.0E-9) at proton energies of 24 and 50 MeV, respectively. To measure the calculated yield, relation (13) can be applied [24]. The results concerning the stopping power and the yield are illustrated in Fig. 9 and are well consistent with the current reports [39, 40].

4. Conclusions

In this work, selenium is used as a target to produce bromine isotopes $^{75}_{35}$Br, $^{76}_{35}$Br, $^{77}_{35}$Br, and $^{80}_{35}$Br for

medical applications. The cross-sections as a function of the proton energy in the production of radioactive bromine nuclei on the selenium-enriched target from 2.00 up to 84.00 MeV are calculated. By comparing the experimental and theoretical results, we have found that the cross-sections are successful in reproducing the experimental data. It can be indicated also that there is a good consistency with previous studies. The reaction of ^{78}Se(p,2n)^{77}Br gives the highest yield for the production of the ^{77}Br isotope. In the field of imaging techniques, the use of these isotopes has increased on the medical side and is likely to continue in the following years.

As a recommendation for future works, (1) bromine isotopes can be produced via more efficient methods by deuteron-induced reactions on krypton; (2) Studying the (p,γ) reaction cross-section; (3) studying the direct and indirect cross-sections.

The authors would like to acknowledge the Ministry of Higher Education & Scientific Research/University of Kerbala in Iraq for the access to research facilities and the support.

1. A.A. Alharbi, A. Azzam, M. M. Cleskey, B. Roeder, A. Spiridon, E. Simmons, V.Z. Goldberg, A. Banu, L. Trache, R.E. Tribble. Medical radioisotopes production a comprehensive via proton induced nuclear reactions on ^{nat}Mo. *Radioisot.–Appl. Bio-med. Sci.* **36** (7) 953 (2011).
2. D. Updegraff. S.A. Hoedl, Ph.D. *Nuclear Medicine without Nuclear Reactors or Uranium Enrichment* (Center for Science, Technology, and Security Policy American Association for the Advancement of Science, 2013).
3. G. Stocklin. Molecules labeled with positron emitting halogens. *Int. J. Rad. Appl. Instrum. B* **13** (2), 109 (1986).
4. H.J. Tochon, J.I. Sachinidis, J.G. Chan, A.M. Scott. *Radiopharmaceuticals in Positron Emission Tomography* (Centre for PET and Ludwig Institute for Cancer Research, Repatriation Medical Centre, 1993).
5. J.F. Ziegler. *Handbook of Stopping Cross-Sections for Energetic Ions in All Elements* (The stopping and ranges of ions in matter, 1980), Vol. 5 [ISBN: 0-08-021607-2].
6. J.F. Ziegler. *Stopping and Ranges Elements* (Helium pergamum press, 1977), Vol. 4.
7. M.U. Khandaker, G. Kim, K. Kim, D. Son. *Experimental Studies of Proton Induced Reaction Cross-Sections on ^{nat}Mo* (Pohang accelerator laboratory, Pohang university of science and technology, 2005).
8. H.H. Lindhard, M. Schardff. *Hydrogen Stopping Powers and Ranges in All Elements* (Stopping Powers and Ranges of Ions in Matter 1961), Vol. 3 [ISBN: 0-08-021605-6].
9. V. Tolmachev, J. Carlsson, H. Lundqvist. Limiting factor for the progress of radionuclide based diagnostics and therapy availability of suitable radionuclides. *Phys. Medd.* **43** (3), 264 (2004).
10. C.J. Anderson, T.S. Pajeau, W.B. Edwards, E.L. Sherman, B.E. Rogers, M.J. Welch. In vitro and in vivo evaluation of copper-64-octreotide conjugates. *J. Nucl. Med. B* **36** (12), 2315 (1995).
11. H.H Andersen, J.F.Ziegler. *Hydrogen Stopping Powers and Ranges in All Elements* (Pergamon Press, 1977), Vol. 9.
12. H.A. Beth, F. Bloch. New cross sections and intercomparison of Proton monitor reactions on Gallium. *Phys. Rev.* **16**, 285 (1933).
13. F.S. Thomas, E.B. Sandor, T.F. Tarkanyib, E. Tavanoa. Evaluated cross section and thick target yield data bases of Zn + p processes for practical applications. *Appl. Rad. Isotopes* **49** (8), 1005 (1998).
14. V.Ya. Nukulin S.N. Polukhin. Saturation of the neutron yield from yergajoule plasma focus facilities. *J. Plasma Phys.* **33** (4), 304 (2007).
15. K.H. Beckurts, K. Wirtz. *Neutron Physics* (Springer, ebook, 1964), Vol. 13 [ISBN: 978-3-642-87614-1].
16. W.B. Amian, R.C. Byrd, C.A. Goulding, M.M. Meier, G.L. Morgan, C.E. Moss, D.A. Clark. Differential neutron production cross sections for 800 MeV protons. *Nucl. Phys. A* **39** (110), 78 (2017).
17. Y. Feige, B.G. Olthman, J. Kasiner. Production rates of neutrons in soils due to natural radioactivity. *J. Geophs. Res.* **73**, 3135 (1968).
18. G.F. Knoll. *Radiation Detection and Measurement* (John Wiley-Sons, 2010), Vol. 7 [ISBN: 978-0-470-13148-0].
19. A.M.J. Paans, J. Welleweerd, W. Vaalburg, S. Reiffers, M.G. Woldring. Excitation functions for the production of bromine-75: A potential nuclide for the labelling of radiopharmaceuticals. *Intern. J. Appl. Radiation and Isotopes* **31** (5), 267 (1980).
20. Z. Kovacs, G. Blessing, S.M. Qaim, G. Stocklin. Production of ^{75}Br via the ^{76}Se(p, 2n)^{75}Br reaction at a compact cyclotron. *Intern. J. Appl. Radiation and Isotopes* **36** (8) (1985).
21. V.N. Levkovskij. Activation cross section nuclides of average masses (A = 40–100) by protons and alpha-particles with average energies (E = 10–50 MeV). *Levkovskij, Act. Cs. By Protons and Alphas, Moscow* **28** (9), 589 (1991).
22. I. Spahn, G.F. Steyn, C. Vermeulen, Z. Kovacs, F. Szelecsenyi, H.H. Coenen, S.M. Qaim. New cross section measurements for production of the positron emitters ^{75}Br and ^{76}Br via intermediate energy proton induced reactions. *Radiochimica Acta.* **97**, 535 (2009).
23. H.E. Hassan, S.M. QaimaYuShubin, A. Azzam, M. Morsy H.H. Coenen. Experimental studies and nuclear model calculations on proton-induced reactions on ^{nat}Se, ^{76}Se and ^{77}Se with particular reference to the production of the medically interesting radionuclides ^{76}Br and ^{77}Br. *Appl. Radiation and Isotopes* **60** (6), 899 (2004).
24. A.G.M. Janssen, R.L.P. Vanden, J.J.M. Degoeij, H.M.J. Theelen. The reactions^{77}Se(p,n) and ^{78}Se(p,2n) as

production roues for ^{77}Br. *Appl. Radiation and Isotopes* **31**, 405 (1980).
25. C.H. Johnson, A. Galonsky, C.N. Inskeep. Cross sections for (p,n) reactions in intermediate-weight nuclei Oak ridge national lab. *Reports* **8** (29), 25 (1960).
26. I. Fedorets, V.D. Zabolotnyi, I.I. Zalyubovskii V.M. Mishchenko, V.E. Storizhko. The levels of ^{77}Br from the ^{77}Se(p, n)^{77}Br reaction. *Izvestiya Akademii Nauk. Ser. Fizicheskay* **41** (8), 16 (1977).
27. E.A. Skakun, V.G. Batij, J.N. Rakivnenko, V.A. Lucik, I.A. Romanij. Cross section ratios for producing isomeric pairs of ^{77m,g}Br^{77}, hadrons ^{80m,g}Br and ^{82m,g}Br in (p,n) reactions. In: *30th Conference, Nucl. Spectra. and Nucl. Struct., Leningrad* (1980).
28. E.A. Skakun, V.G. Batij. Level density parameters from excitation cross sections of isomeric states. *Zeitschrift fur Physik A, and Nuclei* **344**, 13 (1992).
29. I. Spahn, G.F. Steyn, C. Vermeulen, Z. Kovacs, F. Szelecsenyi, M.M. Shehata, S. Spellerberg, B. Scholten, H.H. Coenen, S.M. Qaim. New cross-section measurements for the production of the Auger Electron ^{77}Br and ^{80m}Br. *J. Radiochimica Acta* **98** (12), 13 (2010).
30. J.P. Blaser, F. Boehm, P. Marmier, P. Scherrer. Anregungs functionen und Wirkungs querschnitte der (p,n)-reaction. *Nucl. Phys.* **14**, 14 (1951).
31. C.H. Johnson, C.C. Trail, A. Galonsky. Thresholds for (p, n) reactions on 26 intermediate-weight nuclei. *Phys. Rev. J. Archive* **136** (6B), 22 (1964).
32. S. Kailas, S. Saini, M.K. Mehta, N. Veerabahu, Y.P. Viyogi, N.K. Ganguly. Isobaric analogue resonances in the ^{80}Se(p,n)^{80}Br reaction. *Nucl. Phys. A* **315** (2), 157 (1979).
33. H. Salman, B. Oruncak, R. Unal. Calculation of reaction cross sections for producing Br-75 in the energy range of 5–40 MeV. *Acta Phys. Polon. A* **128**, 224 (2015).
34. I. Spahn, G.F. Steyn, C. Vermeulen, Z. Kovacs, F. Szelecsenyi, H.H. Coenen, S.M. Qaim. New cross section measurements for production of the positron emitters ^{75}Br and ^{76}Br via intermediate energy proton induced reactions. *Radiochim. Acta* **97**, 535 (2009).
35. H.H. Coenen. New radio halogenationmethods. In: *Progress in Radiopharmacy.* Edited by P.H. Cox, S.J. Mather, C.R. Lazarus (1986), p. 196.
36. R.B. Firestone. *Table of Isotopes. CD ROM. 8th* (Wiley Interscience, 1996).
37. H.E. Hassan, S.M. Qaim, Yu. Shubin, A. Azzam, M. Morsy, H.H. Coenen. Experimental studies and nuclear model calculations on proton-induced reactions on ^{nat}Se, ^{76}Se and ^{77}Se with particular reference to the production of the medically interesting radionuclides ^{76}Br and ^{77}Br. *Appl. Radiation and Isotopes* **60** (6), 899 (2004).
38. Ingo Spahn, M.M. Shehata, S. Spellerberg, B. Scholten, H.H. Coenen, S.M. Qaim, G.F. Steyn, C. Vermeulen, Z. Kovacs, F. Szelecsenyi. Investigation of production possibilities of radiobromines for diagnostic and therapeutic applications. *J. Korean Phys. Soc.* **59**, 25 (2011).
39. O. Fasoula, G.A. Souliotis, Y.K. Kwon, K. Tshoo, M. Veselsky, S.J. Yennello, A. Bonasera. Production cross sections and angular distributions of neutron-rich rare isotopes from 15 MeV/nucleon Kr-induced collisions: Toward the *r*-process path. *Nuclear Experiment* **21**, 19 (2021).
40. F. Tarkanyi, A. Hermanne, F. Ditroi, S. Takacs, A.V. Ignatyuk, I. Spahn S. Spellerberg. Activation cross section data of deuteron induced nuclear reactions on rubidium up to 50 MeV. *European Phys. J. A* **57**, 21 (2021).

Received 21.10.22

Хамза А. Межер, Кадхім Аль-Аттафі,
Башар Алкотбе, Вісам Н. Хуссейн

ДОСЛІДЖЕННЯ ПОПЕРЕЧНИХ ПЕРЕРІЗІВ ГЕНЕРАЦІЇ ІЗОТОПІВ БРОМУ В РЕАКЦІЯХ, ІНДУКОВАНИХ ПРОТОНОМ

Розглядається генерація ізотопів брому і досліджуються поперечні перерізи ядерних реакцій в мішені, що збагачена селеном. Це важливо для застосування в медицині та в лікуванні випромінюванням. Відомі вісім каналів генерації ізотопів брому: $^{76}_{34}$Se$(p, 2n)$ $^{75}_{35}$Br, $^{77}_{34}$Se$(p, 3n)$ $^{75}_{35}$Br, $^{76}_{34}$Se(p, n) $^{76}_{35}$Br, $^{77}_{34}$Se$(p, 2n)$ $^{76}_{35}$Br, $^{77}_{34}$Se(p, n) $^{77}_{35}$Br, $^{78}_{34}$Se$(p, 2n)$ $^{77}_{35}$Br, $^{80}_{34}$Se$(p, 4n)$ $^{77}_{35}$Br та $^{80}_{34}$Se(p, n) $^{80m}_{35}$Br. Енергія взаємодіючих протонів сягає від порога реакції в інтервалі 2,20–84,20 МеВ і розрахована з використанням активаційної техніки. Розраховані фактори гальмування та вихід реакції з використанням формули Цейглера. Виконано статистичний аналіз повної енергії та поперечних перерізів для кожної реакції. Ці енергії визначено з прийнятною точністю в інтервалах 0,01 МеВ. Як один з найбільш цікавих результатів, відмітимо розрахунок факторів гальмування в мішенях в рамках підходів Цейглера та SRIM.

Ключові слова: поперечний переріз, формула Цейглера, фактор гальмування, збагачена селеном мішень, вихід брому.